INTEGRATION OF TWO LIDAR FLUOROSENSOR PAYLOADS IN SUBMARINE ROV AND FLYING UAV PLATFORMS

Roberta Fantoni, Roberto Barbini, Francesco Colao, Domenico Ferrante, Luca Fiorani and Antonio Palucci

ENEA, Advanced Physics Technologies Department, Via Fermi 45, 00044 Frascati, Italy;
fantoni(at)frascati.enea.it

ABSTRACT

Strategic lines of international organizations have recently converged on the need to have a reliable, distributed, and independent net dedicated to environmental monitoring. In this framework the survey of marine ecosystems, which is a problem of primary importance in ecological control due to the high probability of accidental risks, deserves particular attention. Coastal waters must be considered a major target for this kind of surveillance, with accidental oil-tanker releases, possible unauthorized industrial wastes – including dangerous organic pollutants (PCB, dioxins, PAH) – and anthropogenic discharges (DOM and detergents).

At the ENEA remote sensing laboratory the former development of ship-borne lidar fluorosensors led to the design of submarine and flying payloads. A compact underwater apparatus was realized and already tested in the XVII Italian Antarctic Expedition on the coastal area of the Ross Sea near terra Nova Bay, where the instrument was used as a payload of a Remotely Operated Vehicle (ROV) both from a pack-located station and from a small boat. The technical layout and characteristics of the submarine lidar fluorosensor will be presented and discussed, together with preliminary results collected during immersions. In different marine contests this instrument can be dedicated to various underwater studies (oceanography, marine biology, glaciology, sedimentology) and to the identification of extraneous objects at the sea bottom (industrial wastes, archeological remains) or to the identification of oil spill releases and residuals. A second instrument, currently under development, consists of a lightweight flying payload, to be installed on an unmanned aerial vehicle (UAV) for large sea surface and territory monitoring.

Keywords: lidar fluorosensor, laser induced fluorescence, submarine payload, phytoplankton, CDOM

INTRODUCTION

International organizations recognized the water quality monitoring as one of the main tasks to be supported for the protection of marine environment and coastlines against the risks of accidental or deliberate pollution. Furthermore, during oceanographic and polar surveys, it is of primary importance to follow the superficial distribution and vertical concentration profiles of organic substances and phytoplankton.

Nowadays, laser-based lidar fluorosensor apparatuses are emerging as very reliable tools to remotely collect information on fluorescent targets for sea and land diagnostics purposes. Remote signatures of dispersed impurities, such as crude oils, CDOM (Coloured Dissolved Organic Matter) or phytoplankton, can be extracted in real time from the collected Laser Induced Fluorescence (LIF) signals (1).

The ENEA laser-based lidar fluorosensor mobile laboratory, built and equipped with local and remote instruments for continuous operation in Antarctic waters, has participated in four oceanographic campaigns, the XIII (Dec. 1997, Jan. 1998), the XV (Jan.-Feb. 2000), the XVI (Jan.-Feb. 2001), and the XVIII (Jan.-Feb. 2003) which gave unique opportunities to record thematic maps of surface and subsurface distributions for main parameters (Chl-a and CDOM) (2,3,4,5). In the Ross Sea and along the Southern Ocean transect, crossed from Terra Nova Bay up to New Zealand, different scenarios were revealed. Annual changes and the spatial and temporal evolutions of both

parameters, heavily affected by local environmental forces, could be followed (6). Furthermore, before and after the XVII campaign the same apparatus was installed on board during the oceanographic transect from Italy to New Zealand (November 2001) and return (March 2002), crossing part of the Mediterranean Sea, all Indian Ocean and a small part of the Pacific Ocean between Australia and New Zealand (7,8). The same kind of information was collected on completely different waters, crossing the route of mostly tropical waters.

The harsh Antarctica environment, where extremely dry atmosphere, low temperature, high speed winds, and packs or icebergs are the usual conditions that limit the survey operations, pushes towards the development of autonomous instruments. Therefore the know-how gained in operating the laser-based systems in Antarctica, was applied to develop a lidar fluorosensor payload for submarine investigation (ROV) and to design a new lightweight flying payload for large surface monitoring to be installed on an unmanned aerial vehicle (UAV). The instruments can also be profitably used for superficial and submarine hydrographic surveillance (in case of pipeline or ship wrecks), since oil spills and floating chemicals can be revealed on the surface or down to the seafloor. In this connection, the lidar payloads can supply important complementary data to concurrent surveys by local (video cameras) or remote (sonar, satellite sensors) techniques.

The ROV payload developed is presented here for the first time together with the results obtained in the XVII Antarctic campaign (Dec. 2001, Jan 2002) during test measurements performed both from a pack ice installation and from a small ship-borne platform. The design of the UAV payload (not yet realized) is shortly discussed in view of the expected performances in the Antarctic environment.

METHODS

Lidar fluorosensor range resolved data

As soon as the laser beam impinges on the sea surface and penetrates along a defined optical path in the liquid medium, red shifted signals are generated at the water scattering wavelength and at different fluorescence wavelengths according to the different fluorophores species encountered (CDOM, algal pigments). Range-resolved equations must be written in the case of time-resolved acquisition of signals.

A simplified version of a pulsed monostatic lidar equation is considered here, which in the case of Raman scattering reads (9):

$$P_D^R(\lambda_R, R) = P_l \frac{A_0}{4\pi R^2} \xi(\lambda) N_W \sigma_W(R) e^{-\int_0^R k_T(R')dR'} \frac{1}{k_T(R)} [1 - e^{-k_T \Delta R}] O(R) \qquad (1)$$

where P_D describes the radiation flux in the unit time detected by the receiver at the time $t=2n_w R/c$, P_l is the transmitted power for a laser pulse of duration τ_l, the collective factor $O(R)A_0/R^2$ represents the sensitivity function of the receiver optics, $\xi(\lambda)$ is the receiver's spectral transmission factor, σ_W is the Raman cross section of the W species with N_W number density, $k_T(R) = k(\lambda_l, R) + k(\lambda_R, R)$ is the two way extinction coefficient at range R with contributions at the laser (λ_l) and Raman (λ_R) wavelengths. The fluorescent emission at λ wavelength has a form similar to eq. (1):

$$P_D^F(\lambda, R) = P_l \frac{A_0}{4\pi R^2} \frac{\sigma_{chl}^A(\lambda_l)\phi_F K_0(\lambda)\lambda_l}{\lambda} N_0(R) e^{-\int_0^R k'_T(R')dR'} \frac{1}{k'_T(R)} (1 - e^{-k'_T \Delta R}) O(R) \qquad (2)$$

where $k'_T(R) = k(\lambda_l, R) + k(\lambda, R)$ is the total extinction coefficient at the laser λ_l and fluorescent λ wavelength, $\sigma^A(\lambda_l)$ is the absorption cross section, $K_0(\lambda)$ is an effective spectral filter efficiency.

The problem of inverting eqs. (1) and (2) is fairly complex. In (10) it was demonstrated that, under the assumption of a homogeneous water column and fluorescence lifetimes significantly shorter

than both the laser pulse width and the detector time response for all the fluorophores, it is possible to obtain the range resolved two path extinction coefficient, as:

$$k(\lambda_l, R) + k(\lambda, R) = -\frac{d}{dR} \ln\left[\frac{P_D(R)R^2}{O(R)}\right]$$ (3)

A simultaneous evaluation of eq. (3) for a number of different spectral channels, including the elastic one, allows for determining the extinction coefficient at each selected wavelength.

The lidar fluorosensor payload for ROV – a robust realisation

The first generation of ship-borne lidar fluorosensor apparatuses was dedicated to seawater superficial monitoring, collecting LIF signals in the time integrated mode. In order to obtain information on depth distribution of different substances which stratify in sea-waters, range-resolved measurements become mandatory. The approach requires the entire fluorescent echo of each species to be recorded on fast transient digitisers. Time-resolved fluorescence apparatuses were previously developed to investigate the water column either from ship-borne (11) platform or from ROV (12). In particular, a combined LIF and vision remote sensor has been developed by the Marine Physics Institute of the Carl von Ossietzky University of Oldenburg (D) in order to locate and detect the release of toxic chemicals and to inspect the seafloor (12). Our group also previously developed a prototype installed at the bottom of the oceanographic vessel, looking downward at the water column under the ship (13, download full paper 1300 kB). The system allowed to gain expertise on the range-resolved operation and to optimise the detection electronic chain. The performances of the ship-borne range-resolved prototype were validated by comparing near surface data with concurrent measurements obtained with the surface integrated lidar; the instruments were simultaneously installed on the same boat during the XV Italian Antarctic Mission (3). The performances of the lidar fluorosensor payload presented here are partially based on constraints obtained from the former experiment.

The new submarine lidar fluorosensor was built and tested at the ENEA laboratory of Frascati as an interchangeable package of the Antarctic ROV developed by the Robotic Department of CNR-ISSIA in Genua (14). The optoelectronic components, including a compact Nd:YAG laser operated in 3rd harmonic and the receiver, have been designed in order to fulfill the highly demanding ROV requests in terms of roughness, weight, size, and power consumption, which allowed it to operate in different scenarios, either in Antarctic Sea or in the Mediterranean Sea. Valuable technological improvements in hardware, optics, electronics, and acquisition software were necessary to design and build the ROV payload, having many constraints on ruggedness and reliability.

Particular care has been devoted to reduce the weight and size of all lidar subsystems, to minimise the power requirements for laser operation and to achieve thermal stability with respect to the extreme environmental temperatures. Details of the achieved project requirements are discussed in the following, while technical parameters are given in Table 1.

Following ROV constraints (12), the payload, designed to scan a water column down to 300 m depth, has a maximum allowed weight of approximately 150 kg. Its overall size cannot exceed the ROV frame, in order to prevent possible damages during the submarine diving. The ROV with its payload is secured to the surface control station by a 500 m long submarine cable also used for supplying main power to the instruments and for data transmission through a fiber optic F/O. The frame of the lidar payload consists of a stainless steel cage, supporting two titanium cylinders, each 300 mm in diameter and 1,100 mm long. The detailed characteristics of the apparatus are listed in Table 1, while its schematic diagram is shown in Figure 1.

Table 1: Main characteristics of the lidar fluorosensor components installed in the ROV payload.

Transmitter	Q-Switched Nd:YAG laser II and III
Energy	70 mJ/pulse, 10 ns @ 355nm
Ppr	10 Hz
External size	190 mm (large), 150 mm (height), 800 mm (length)
Photodiodes	3 (1064 nm, 532 nm, 355 nm) laser emission, 1 (532 nm) optical trigger (delay 20ns, jitter 3 ns)
Expander	Variable (3x)
Detectors	Hamamatsu PMT R-1924 (2), R-1925 (2)
Motors	Harmonic controls
Filters	Dichroic T>90% (@ 400 nm)
	Interferential 402, 450, 650, 680 nm ($\Delta\lambda$ = 10nm HWHM)
Telescope	Cassegrain 230 mm diameter, F # 2
Window	Suprasil 3 quartz, 300 mm diameter, 40 mm thick
Optic splitter	Four faced aluminised prisms (base 24.5 x 24.5 mm^2)
Digitizer	Signatec ISA/PCI 500 Ms/s, 8 bit
Monitors	Temperature, Q-switch on/off, HV control, optical signals (3), radiance
Interface	RS232
Computer	Axiom AX6050DWP passive backplane

A modular custom designed Nd:YAG laser is lodged inside one of the Ti cylinders of Figure 1 within an internal aluminum cage which also hosts the high voltage power supply and heat exchanger, in a mounting which allows their easy extraction for adjustments and service. Second and third harmonic frequency multiplication is achieved in the laser head by means of BBO crystals. Pulse energies emitted both at the fundamental and harmonics wavelengths are monitored by three photodiodes (PD1-3), which are used to optimise the crystals conversion efficiency by tilting them through the corresponding computer-controlled actuators (M). The overall power consumption of the apparatus, with the laser running, resulted to be about 600 W.

The thermal stability is a main concern for operation in Antarctica, due to the very large excursions in environmental temperatures, ranging from -2°C in the seawater, down to -40°C outside and up to 5-15°C inside the host platforms. A water-air heat exchanger between the laser head and the surroundings is included for temperature regulation. A fan connected to the heat exchanger assures a proper airflow circulation inside the cylinders and the onset of suitable conditions for operation of all the electronic equipment. Two thermal sensors are placed close to the laser head (T1) and near the electronic control devices (T2), in order to continuously monitor the internal temperature. An internal constant regime of 20°C is reached after about 30 minutes of laser operation with -4°C outside.

In order to prevent freezing and damages of the laser components during hardware transfers, the internal water cooling system can be evacuated through the input/exhaust connections of the hosting cylinder.

The generated laser beam is expanded and directed to the second cylinder (Figure 1), through a small connecting pipe, where it leaves the system coaxially with the receiving optics. This cylinder also hosts four PMTs detectors, the preamplifiers, and the computer. It is closed by a large quartz window which allows for the transmission of both the outgoing laser beam and the incoming seawater's backscattered optical radiation. Optical trigger is generated by a dedicated photodiode (PD4).

A compact mounting was designed for the collecting optics, in order to include both the telescope and the PMTs in a common shielded case. A CAD optical ray-tracing programme has been used to optimise the optical transport of the signals received from the water to the four channel detectors. Optical elements include a Cassegrain telescope (220 mm aperture), a field stop, a collimat-

ing lens and a fully reflecting prism splitting the radiation towards the PMT detectors equipped with appropriate interference filters for wavelength selection. The prism has been custom realized with aluminized surfaces in order to minimize the optical path and to split the received radiation into four equivalent branches. Additionally, to trace the occurrence of occasional sensitivity variations during the field operation, a red light emitting diode (PD5) is used to give a constant reference pulse of known duration and intensity. Its optical output is coupled with a four-branch 500 μm plastic fibre optics, whose ends are placed directly in front of the PMTs. The duration and time position of reference pulses are completely software controlled and can be generated between consecutive laser pulses. After being detected by the PMTs at the selected wavelengths, the LIF signals are digitised by four-channel fast ADC converters.
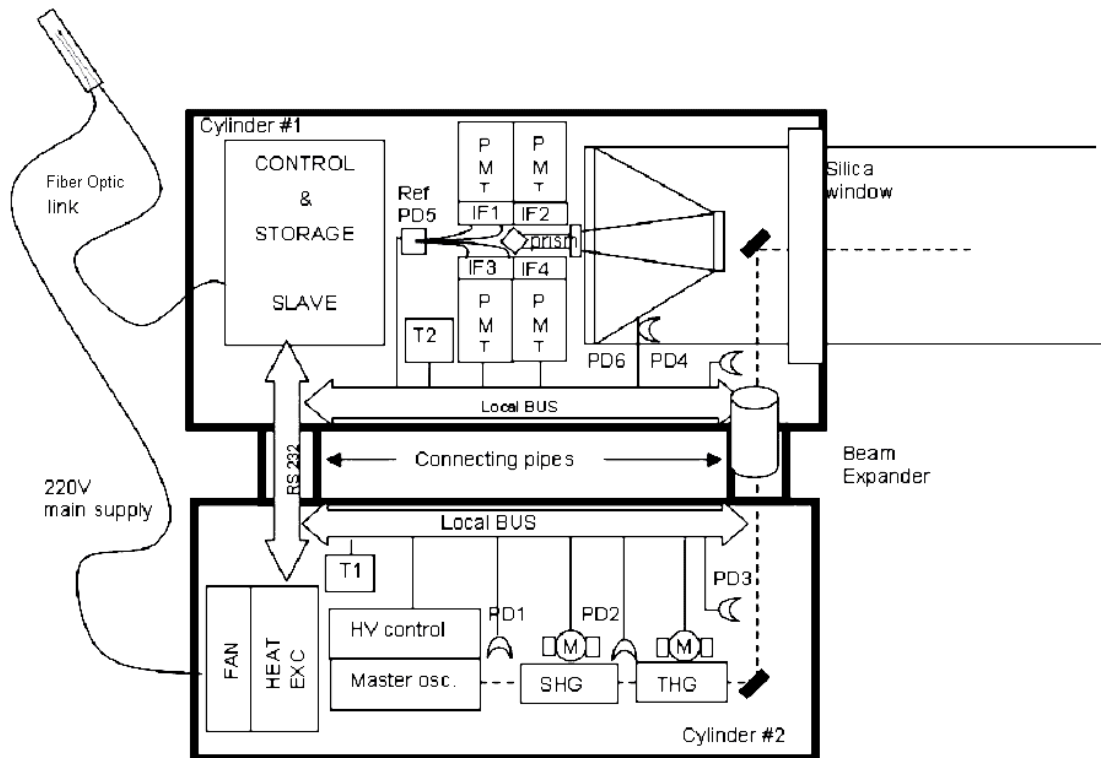

Figure 1: Schematic layout of the lidar payload: PMT (1-4) photomultipliers; IF (1-4) interference filters; PD (1-3) laser emitting photodiodes; PD4 optical trigger photodiode; PD5 emitting reference photodiode; PD6 PAR photodiode; M stepping motor; T trigger signal.

The total radiance, expressed in μmol quanta m^{-2} s^{-1}, impinging onto the collecting optics during the immersion can be measured by a calibrated photodiode (PD6) placed behind the quartz window.

All the subcomponents are optimised for underwater operation: the optical elements of the telescope are adjusted so that the collection efficiency reaches a constant value within the first ten meters. An incomplete knowledge of the lidar collection efficiency can significantly affect the optical properties retrieved by this kind of apparatuses, especially in the near field range, where the signal can saturate the detector. To this respect, we adopted a calibrated fluorescent target to experimentally estimate the collecting optic efficiency prior to underwater operation.

An industrial PC, hosting PCI/ISA slot cards, controls all the experimental settings, as well as the acquisition and temporary data storage. All control signals from laser source, including the high voltage power supply, Q-switch and laser controls are acquired by the local computer through an RS232 interface. The system in its present version is able to collect data from four channels simultaneously, sustaining an acquisition data rate of 10 laser shots per second.

The control, at the surface station, is maintained via an Ethernet F/O link between the master (surface) and slave PC (submersible). The F/O cable allows for broadband transmission of up to four video channels for visual inspection of the sea bottom and for fast Ethernet connection. A dedicated software has been developed to monitor in real time all the experimental settings and to make changes in the operating parameters (i.e. laser or PMTs HV, amplifier gain, number of averages).

A proper synchronization between LIF signal and laser pulse is accomplished by an accurate optical trigger, generated by a reference photodiode (PD5). The required conversion time is about 100 µs, after which the lidar profile corresponding to each laser shot is placed in a temporary memory storage and accumulated until the fixed number of laser shots is reached. Data are then compressed and sent to the surface base via a communication channel. Critical parameters such as temperature and high voltage are continuously monitored by the master station.

The lidar fluorosensor payload for UAV – an ambitious design

In Antarctic regions, or in an ecological disaster scenario, crew safety is a challenging issue due to a very limited assistance from navigation aids or en route radar, while dramatic weather changes can occur with quickly shifting winds, and visibility and ceiling dropping to zero. The use of a relatively low-cost, uninhabited VTOL (vertical take-off and landing) aerial vehicle, operated by a small crew from a ship, to survey marine or terrestrial ecosystems can therefore be attractive. In fact this aerial vehicle can compensate for the limited ship or van and, more important, substitute manned helicopters where they cannot fly (e.g. over the open sea in Antarctica or in case of ecological disasters). In this respect, a flying lidar fluorosensor payload is under development to be used in conjunction with a lightweight UAV in order to investigate coastal sites of special biological interest or high-risk areas.

The UAV carrier, already in an advanced stage of development at the Polytechnic of Turin and at the University of Rome "La Sapienza" (14), is shown on the left side of Figure 2. It has a maximum takeoff force of 1000 N. The shroud diameter and height are 1.9 m and 0.6 m, respectively. The shroud encloses the rotor hub mechanics and engines and hosts the control electronics and navigation devices.

In designing the flying lidar payload, valuable technological improvements in hardware are required to stay within the UAV operation limits. The actual efforts are mainly concentrated to reduce the load (below 10 kg) and size of all the lidar subsystems as well as to keep to a minimum the electrical power requirements (not exceeding 600 W) for laser and electronics operation.

One or two sections of the UAV will be used to host a compact diode-pumped solid state laser, equipped with a third or fourth harmonic UV generator (Figure 2, right side). This source was chosen for the light and rugged structure as a transmitter. The receiver will be formed by a Fresnel PVC lens focusing on miniaturised detectors. A PC will be employed for controlling and operating the system. Common ancillary instruments such as GPS, and flight data, namely roll and pitch attitude, will be shared with the UAV instruments, and their data will be transmitted to the lidar PC through a RS-232 serial interface, in order to produce fluorescence thematic maps of the investigated areas. In a typical mission scenario, the UAV flies over a 10 x 10 km^2 area at an altitude of 20 m. The mission of the LIF payload will be addressed to monitor surface waters (sea, lake, river) with an expected depth penetration in the order of a few meters, no time resolved technique will be implemented in the flying prototype. If we hypothise that the scanned area sides are oriented north and east, the vehicle will fly, every 2 km in the north direction, 10 km long straight segments alternately heading east or west. At the end of the mission, the duration of which is well within the considered 2 hours endurance, the vehicle is recovered onto the ship.
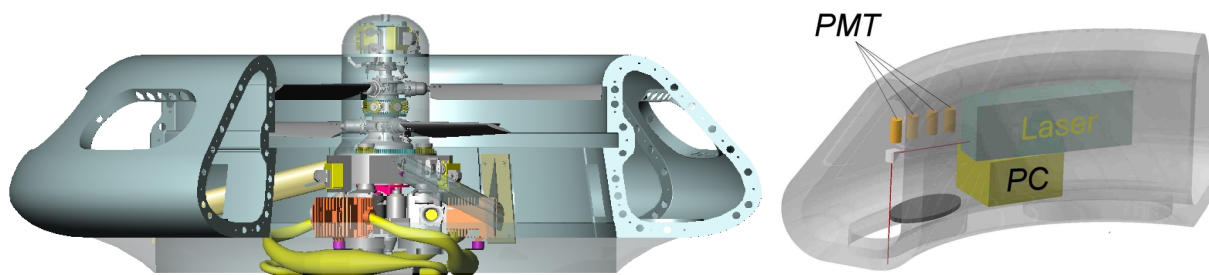
Figure 2: The UAV and its payload. Left: Interior view with rotor hub mechanics and engines; Right: Schematic of the lidar fluorosensor payload with its main components

RESULTS

The ROV mounted lidar has been first tested during the XVII mission (Dec. 2001 – Jan. 2002) in Antarctica, at locations close to the Italian base of Terra-Nova Bay (TNB), by driving the submarine carrier along vertical and horizontal transects. The command and control station was located either on the ice pack or on a small boat.

The first solution was adopted at the beginning of the Australian summer, when the ice pack still covered the whole TNB area. A tent was used to protect master and slave instrumentation, while the ROV was immersed in the underlying water through a hole drilled through the ice. After the ice-break, which occurred in the full summer season, the ROV was operated from aboard the ship *Malippo*. In this case, the ROV position was retrieved with good accuracy after merging the data supplied by a GPS with a VSBL (Very Short Base Line) Acoustic Positioning System.

In order to properly analyse the range-resolved data collected according to the method discussed above, an accurate knowledge is needed of optical parameters k and n for the used wavelengths. As remarked in (15), a quite large discrepancy is observed among literature data, especially in the short wavelength region, where the contribution of organic compounds becomes important. In the present work changes in temperature and salinity gradients along the investigated water column must be considered as well.
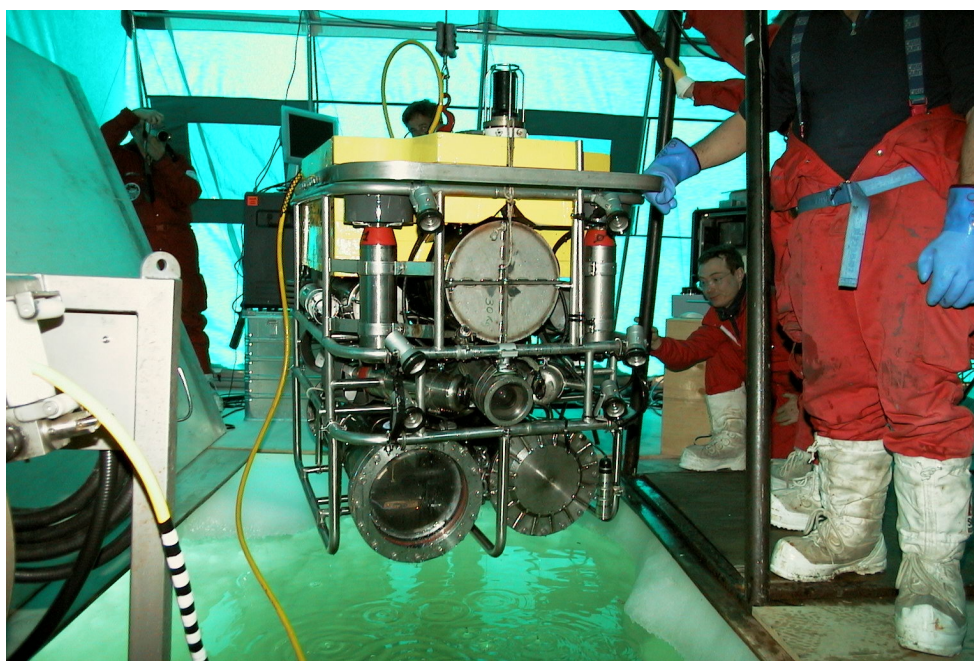

Figure 3: Lidar fluorosensor payload (two cylinders at the bottom of the frame) connected to the ROV, inside the tent during the first Antarctic test (TNB, Dec. 24, 2001).

Figure 4 shows an example of a 5 s average (corresponding to 50 laser shots) of range-resolved horizontal profiles for three simultaneously acquired different channels (Raman, CDOM and Chl-a fluorescence). The integration time choice was consistent with the ROV speed and gave an extremely high spatial resolution of 1 m. The latter offers the chance, once an interesting feature is found, to utilize the submersible vehicle abilities to stop, hover and slowly move around. The observed noise level is consistent with the resolution in acquisition (8 bit). By averaging over 50 laser shots, we observed nearly three orders of lidar signals amplitude dynamic, thus the experimental system is actually performing at the best of its possibilities. Should a larger range be needed, it would be necessary to increase the geometrical compression of receiving optics, in order to shift the signal dynamic towards long distances.
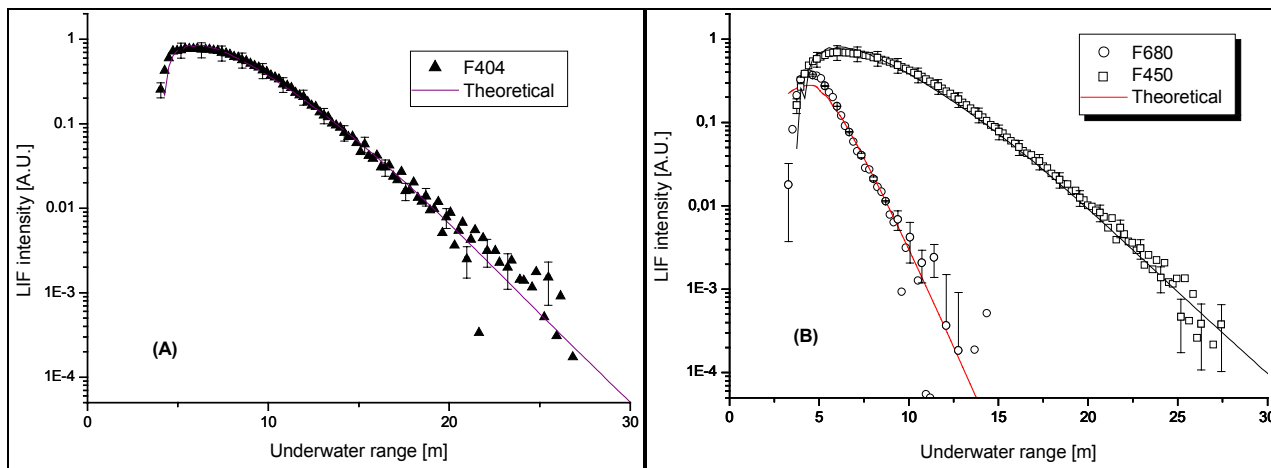

Figure 4: Typical range-resolved LIF signal compared with simulated extinction. Left: 404 nm; Right: 450 nm and 680 nm. [TNB, Dec. 24, 2001].

A complete vertical profile gathered up to the maximum reachable depth of approximately 200 m is shown in Figure 5, as obtained by integrating on the full range, at each underwater quote, horizontal range resolved curves of the kind shown in Figure 3. The range-integrated responses at 404 nm (Raman backscattering) and at 450 nm (CDOM) are reported in Figure 5 (left), while their ratio (CDOM normalized to Raman signal) is shown in Figure 5 (right).
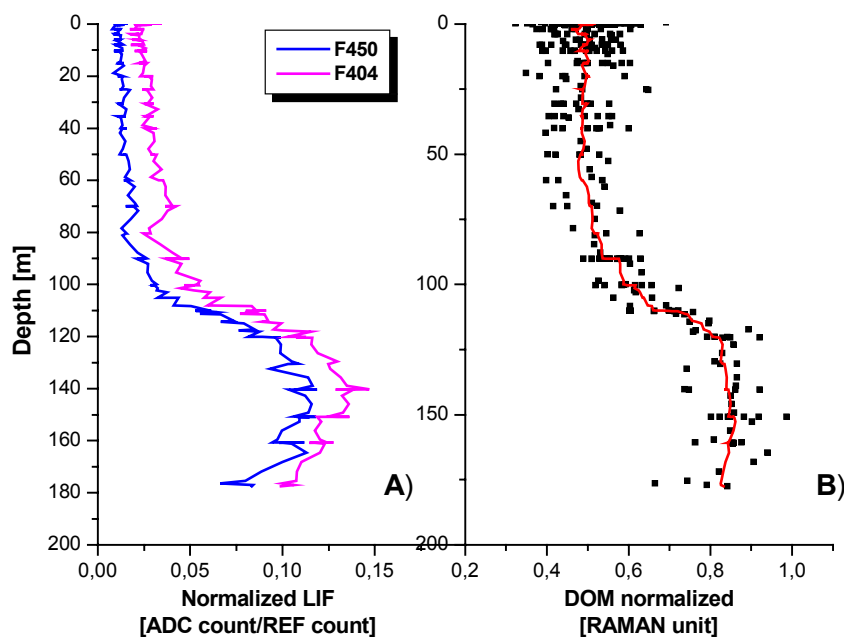

Figure 5: Vertical transect. Behaviour of the integrated LIF signals along the depth: Left: 404 nm and 450 nm; Right: 450 nm signal, Raman normalised [TNB, Dec. 13, 2002].

Minor variations related to water characteristics are detected in all the curves down to about 100 m, corresponding approximately to the lower end of the euphotic zone. At this depth a strong increase emerges in crossing a boundary layer and suggesting the presence of a vertical stratification between the upper and lower seawater levels (16). The observed variation could actually be related to changes either in the composition of optically active molecules or in CDOM total concentration, while both phenomena may occur together. The increase in the specific spectral emission at 450 nm seems to be related to higher CDOM concentration, since the presence of other non-fluorescent substances in the water column would give rise to higher attenuation, due to absorption phenomena, in the lidar signal.

To clarify this point, inversion of LIF range-resolved signals was performed according to eq. (2), by introducing the measured collecting efficiency of the telescope in order to evaluate the attenuation coefficient. The data set examined was the same as in Figure 5, for which an isolevel 2D plot is reported in Figure 6. The two-way attenuation $k(\lambda_{355}) + k(\lambda_{404})$, computed according to eq. 3, is shown in Figure 6 left, while Figure 6 right corresponds to the case $k(\lambda_{355}) + k(\lambda_{450})$. Once again it is possible to note a higher density of isolines around 90-110 m depth, indicating the presence of a density gradient. At higher depths, we observed a decrease of attenuation thus indicating clearer water for which the effects of scattering (and multiple scattering) is reduced. Although conditions for inversion of lidar signals (9) are satisfactorily matched in the present case of moderately turbid coastal water examined, the assumed linear relationship between CDOM fluorescence and absorption is not obviously valid. An increase of extinction with depth is indeed expected and partially observed in Figure 6, probably related to both the presence of attenuating non-fluorescing substances at higher depths and the occurrence of particle scattering near the surface.
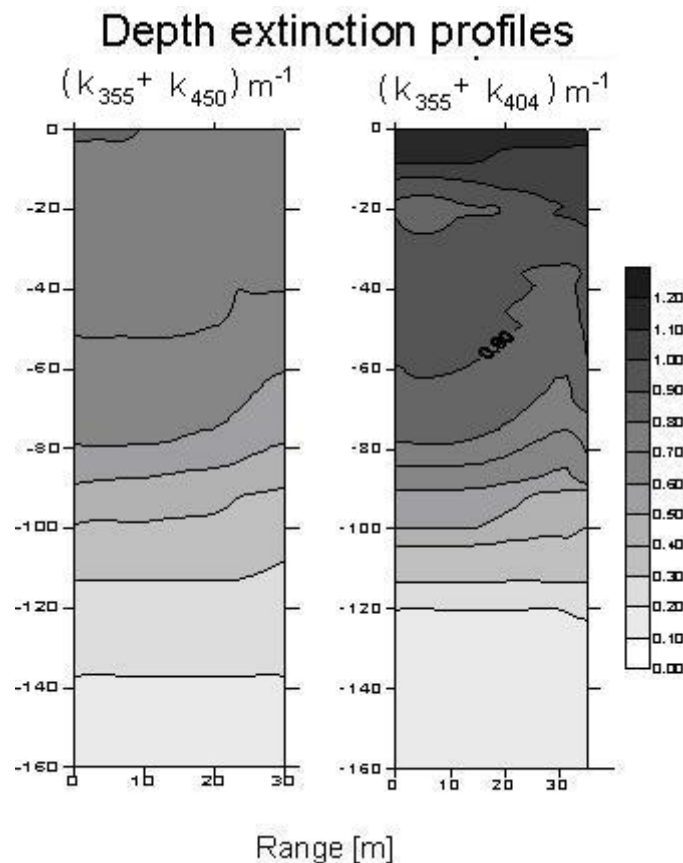

Figure 6: Retrieved extinction profiles of Figure 5: Left: $(k_{355} + k_{450})$ m^{-1}; right: $(k_{355} + k_{404})$ m^{-1}.

DISCUSSION

The range-resolved system resulted to be suitable to gain high-resolution information on water stratification along a deep water column. Whatever is the physical origin of the phenomenon observed by the new submersible instrumentation, the well-defined vertical structure found in this experiment does not appear unexpectedly. It is indeed well known that a stratification within the first few tens of meters and up to one hundred may typically occur in Antarctic coastal water, as inferred from local sampling and different probe measurements (15).

In comparing the results achievable by the range-resolved submarine payload to different conventional or lidar instrumentation suitable to investigate water columns, we can stress unique performances of the new device. Formerly developed ship-borne range resolved instrumentation had a limited penetration depth, which confined their use to the upper part of the photic layer during the cruise. Conversely, conventional instruments, such as CTD, require a ship stop for deploying and reloading, and cannot operate along the water column during navigation. *In situ* determination obtained with CTD were already successful compared with range-resolved lidar transects in the Antarctic Ross Sea (13). The ROV operated range-resolved system is characterised by a short investigated range (10-20 m), but is capable of moving along horizontal or vertical transects. In particular the information collected horizontally at different levels of the water column is unique to map three-dimensionally the water stratification and model the full water mass crossed.

CONCLUSIONS

A submarine lidar fluorosensor, designed and built for remotely monitoring marine ecosystems and tracing sea water pollutants, was successfully tested during the XVII Antarctic campaign in which it was operated from a ROV. The success of site tests (temperature, pressure, electronic compatibility and power supply) allowed to operate the instrument down to 180 m depth in the harsh Antarctic environment.

During vertical immersion paths, the lidar fluorosensor payload was able to collect horizontal range-resolved data relevant to different biochemical features (CDOM, Chl-a). The capability of the instrument to trace parameters in deep subsurface waters, not reachable from surface systems, was demonstrated. Data analysis, based on models using current theoretical background and known optical properties, appeared feasible and allowed to obtain preliminary results.

The kind of data collected by the lidar fluorosensor submersible payload are of interest to marine biologists involved in determination of photosynthetic activity and total biomass productivity, and to chemists addressed to impurities recognition and quantitative analysis. Results of systematic investigations performed by submersible lidar fluorosensor payloads could be profitably used also by researchers involved in oceanography, glaciology, and sedimentology aimed at characterizing the Antarctic environment, which includes studies of water mass formations and dynamics under ice tongues and of ice melting effects.

A complementary lidar fluorosensor payload for surface investigation from remotely piloted flying vehicles was also designed, in order to obtain information on sea-water parameters on a spatial range broader than that crossed by the research vessel utilised in Oceanographic campaigns.

ACKNOWLEDGEMENTS

REFERENCES

1   Panne U, 1998. Laser remote sensing. <u>Trends in Analytical Chemistry</u>, 17: 491-500

2   Barbini R, R Fantoni, F Colao, A Palucci & S Ribezzo, 2001. Differential lidar fluorosensor system used for phytoplankton Bloom and sea water quality monitoring in Antarctica. <u>International Journal of Remote Sensing</u>, 22: 369-384

3   Barbini R, F Colao, R Fantoni, G M Ferrari, A Lai & A Palucci, 2003. Application of a lidar fluorosensor system to the continuous and remote monitoring of the Southern Ocean and Antarctic Ross sea: results collected during the XIII and XV Italian oceanographic campaigns. <u>International Journal of Remote Sensing</u>, 24: 3191-3204

4   Barbini R, S Ceradini, F Colao, R Fantoni, G M Ferrari, A Palucci, S Sandrini, L Tositti & O Tubertini, 2003. Simultaneous measurements of remote lidar chlorophyll and surface CO_2 distribution in the Ross Sea. <u>International Journal of Remote Sensing</u>, 24: 1-13

5   Barbini R, F Colao, R Fantoni, L Fiorani, M Galli & A Palucci, 2003. Remotely sensed primary production in the western Ross Sea: Results of *in situ* tuned models. <u>Antarctic Science</u>, 15: 77-84

6   Nieke B, W F Vincent, J C Therriault, L Legendre, J F Berthon & A Condal, 1997. Use of a Ship-Borne Laser Fluorosensor for Remote Sensing of Chlorophyll a in a Coastal Environment. <u>Remote Sensing of Environment</u>, 60: 140-152

7   Artamonov E S, F Colao, L Fiorani & A Palucci, 2002. Calibration and validation of satellite data with the ENEA lidar fluorosensor during the MIPOT oceanographic campaign. <u>ENEA Technical Report</u> RT/2002/28/FIS

8   Barbini R, F Colao, L De Dominicis, R Fantoni, L Fiorani, A Palucci & E S Artamonov. Analysis of simultaneous chlorophyll measurements by lidar fluorosensor, MODIS and SeaWiFS. Submitted to <u>International Journal of Remote Sensing</u>

9   R Measures, 1977. Lidar equation analysis allowing for target lifetime, laser pulse duration and detection integration period. <u>Applied Optics</u>,16: 1092-1103

10   Harsdorf S & R Reuter, 1999. Laser remote sensing in highly turbid waters: validity of the lidar equation. <u>SPIE</u>, 3821: 369-377

11   Ohm K, R Reuter, R Willkomm & M Stolze, 1998. Shipboard oceanographic fluorescence lidar development and evaluation based on measurements in the Antarctic waters. <u>EARSeL Advances in Remote Sensing</u>, 5: 104-113

12   Harsdorf S, M Janssen, R Reuter, S Toeneboen, B Wachowicz & R Willkomm, 1999. Submarine lidar for seafloor inspection. <u>Measurement Science and Technology</u>, 10: 1178-1184

13   Barbini R, F Colao, R Fantoni, A Palucci & S Ribrezzo, 2001. Range resolved lidar fluorosensor for marine investigation. EARSeL eProceedings, 1(1): 175-184

14   Veruggio G, M Caccia & R Bono, 1997. ROMEO: a multi-role unmanned underwater vehicle for advanced robotics developments. <u>Proceed. of 4th International Symposium on MMAR97 Methods and Models in Automation and Robotics</u> (Miedzyzdroje, Poland), 2: 517-522

15   Litjens R A J, T I Quickenden & C G Freeman, 1999. Visible and near-ultraviolet absorption spectrum of liquid water. <u>Applied Optics</u>, 38: 1216-1223

16   Fabiano M, P Povero & C Misic, 1999. Spatial and temporal distribution of particulate organic matter in the Ross Sea. F M Faranda, L Guglielmo & A Ianora (Eds.). In <u>Ross Sea Ecology</u> (Springer Verlag, Berlin) 135-149